Journal of Magnetism and Magnetic Materials 372 (2014) 173–180

Contents lists available at ScienceDirect

Journal of Magnetism and Magnetic Materials

journal homepage: www.elsevier.com/locate/jmmm

Phase diagram and reentrance for the 3D Edwards–Anderson model using information theory

V. Cortez [a], G. Saravia [b], E.E. Vogel [b,*]

[a] Facultad de Ingeniería y Ciencias, Universidad Adolfo Ibáñez, Avenida Diagonal las Torres 2640, Peñalolén, Santiago, Chile
[b] Departamento de Ciencias Físicas, Universidad de La Frontera, Casilla 54-D, Temuco, Chile

ARTICLE INFO

Article history:
Received 17 April 2014
Received in revised form
20 July 2014
Available online 7 August 2014

Keywords:
Edwards–Anderson model
Lattice theory
Spin-glass

ABSTRACT

Data compressor techniques are used to study the phase diagram of the generalized Edwards–Anderson model in three dimensions covering the full range of mixture between ferromagnetic (concentration $1-x$) and antiferromagnetic interactions (concentration x). The recently proposed data compressor wlzip is used to recognize criticality by the maximum information content in the files storing the simulation processes. The method allows not only the characterization of the ferromagnetic to paramagnetic (FP) transition ($x<0.22$, or $x>0.78$) but also it equally well yields the spin-glass to paramagnetic (SP) transition ($0.22<x<0.78$). A reentrance of a ferromagnetic phase into the spin-glass phase is found in the vicinity of the multicritical point. The differences in the ways to apply the new method to FP and SP transitions are reported. A phase diagram for the entire range of x based entirely on the use of compression techniques is obtained and discussed. The advantages and disadvantages of the method of data compression as compared to other methods to deal with magnetic phase transitions are brought out and explained.

1. Introduction and motivation

Phase transitions of ferromagnetic to paramagnetic regimes can be characterized in a number of ways for fixed-point systems. However, less techniques are available for complex systems where the ground manifold is disconnected and spread over many "valleys" in the configuration space, which is usually full of metatstable states acting as traps for any dynamics. The recent proposal of a method based on information theory [1], namely, data compression techniques applied to obtain the phase diagram of 2D diluted ferromagnets, opens a new possibility to deal with these problems. In particular the proposal of a new data compressor, named wlzip [2], allows to improve the determination of critical temperatures. This is just another example of the expanding universe of applications of information theory to different branches of science [3–5].

In the present paper we address the phase diagram of the generalized three-dimensional Edwards–Anderson (EA) model: the starting point is the 3D Ising ferromagnet in which a proportion x of the nearest neighbor interactions (the only ones considered here) are successively replaced by antiferromagnetic interactions of the same strength. The full range for x is considered (symbol $1-p$ is sometimes used in the literature to represent this concentration). For the cubic lattices to be used in the simulations below the situation is symmetric with respect to the point $x=0.5$. This particular concentration corresponds to the usual EA model in 3D, a case vastly considered in the literature since the pioneer work by Ogielski and Morgenstern [6].

The phase diagram has also been studied by different authors using a variety of methods. An initial proposal can be found in the work of Ozeki and Nishimori [7] up to some recent ones [8]. In spite of this effort, some points still require complementary results and independent analyses; such is the case of the possible reentrance proposed for this system [9] and even for the 2D $\pm J$ Ising model [10]. In the present paper we present the most complete phase diagram showing reentrance for the 3D generalized EA model. However the main aim of the present work is to introduce a new and independent method based on information theory to look into this problem with some advantages.

The usual crossing methods [1] give a clear transition temperature for concentrations $x<0.22$. This is illustrated in Fig. 1 for the particular concentration $x=0.125$ (details will be discussed later on). However, the same methods cannot equally resolve transitions for $x>0.22$ (Fig. 2, for $x=0.375$) although other techniques recognize a spin glass to paramagnetic transition for these concentrations of AF bonds [8]. Can the method based on data compression recognize this second phase transition as well? We present here the first attempt to extend this method to 3D Edwards–Anderson systems. The application of this method to 2D EA systems yielded the recognition of the ferromagnetic to

* Corresponding author.

http://dx.doi.org/10.1016/j.jmmm.2014.07.055
0304-8853/

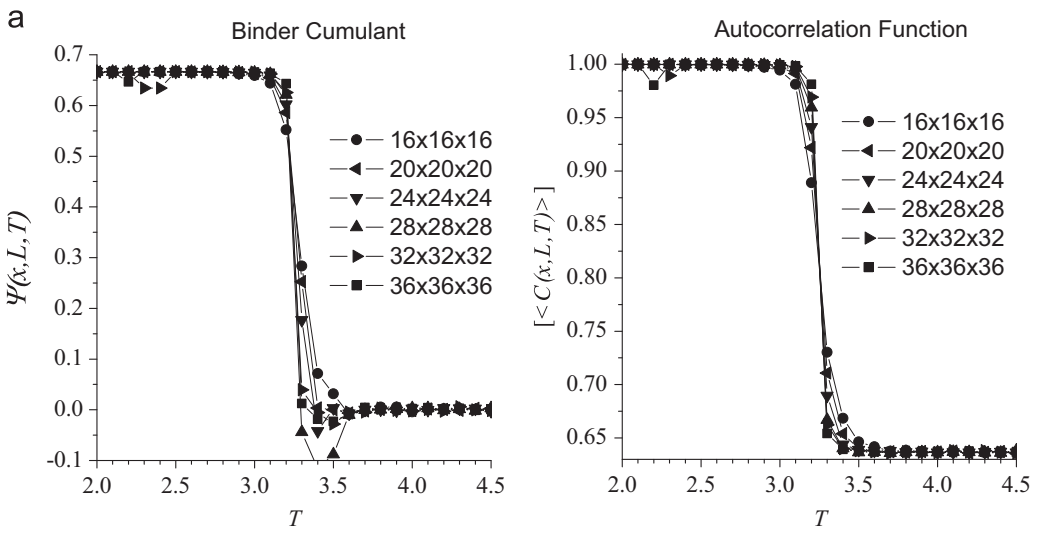

Fig. 1. Determination of the critical temperature for concentration $x=0.125$, by means of two crossing mechanisms: Binder cumulants (left) and autocorrelation functions (right); sample sizes are given in the insets. Curves intersect near $T \approx 3.25$.

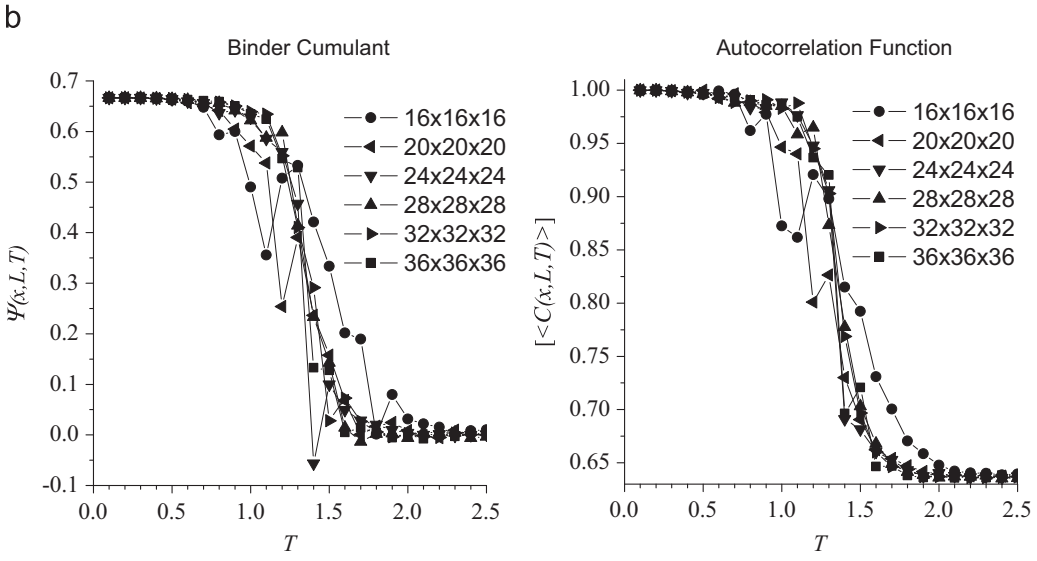

Fig. 2. Attempt to determine the critical temperature for concentration $x=0.375$, by means of two crossing mechanisms: Binder cumulants (left) and autocorrelation functions (right); sample sizes are given in the inset. No single clear intersect is observed. This behavior persists even if equilibration times are increased (not shown).

paramagnetic transition for $x \leq 0.1$ but in such systems there is no ordered phase for $0.1 < x < 0.9$ at any finite temperature. The application of the method of data compression to the 3D EA method done in the present paper is an alternative way to study the phase transitions present here. This also gives us an opportunity to appreciate the differences of the method when applied to ferromagnetic (F) to paramagnetic (P) transitions as compared to spin-glass (S) to paramagnetic transitions.

As this is the first time the method of data compression is applied to the spin-glass to paramagnetic transition we will pay attention to the possible new features appearing here. As we will see, there are differences: F to P transitions produce sharp curves for the information theory indicator while S to P transitions obtained under the same previous precision produce broader curves, thus evidencing a different phenomenon.

In the following section we define the system, Hamiltonian and properties to be measured by means of simulations based on Monte Carlo algorithms. In Section 3 we present and discuss results beginning by revisiting previous results anticipated in Figs. 1 and 2; we continue then by the application of the new method aiming for a well defined full phase diagram including both ferromagnetic to paramagnetic transitions as well as spin-glass to paramagnetic transitions. Section 4 is devoted to conclusions.

2. System, Hamiltonian and parameters

2.1. Review of main definitions

Let us consider a simple cubic lattice with Ising spins S_i at the $L^3 = N$ sites ($i = 1, 2 \ldots N$). Such spins interact among themselves via exchange nearest-neighbor interactions all of the same magnitude $J > 0$, but with random distribution of signs ($\pm J$), with a negative interaction for ferromagnetic (F) interactions and positive for antiferromagnetic (A) interactions. The concentration of A interactions (or bonds) is x; the concentration of F interactions is $1-x$ since no vacancies are allowed. No external magnetic field is

considered here. Then, the Hamiltonian can be written as

$$H = \sum_{[i,j]} J_{ij} S_i S_j, \tag{1}$$

where $[i,j]$ means sum over i considering j over the nearest neighbors to spin S_i; exchange interactions J_{ij} can be either $+J$ (A) or $-J$ (F) according to the previous discussion.

A state is defined here as a set of all S_i's stored in a fixed order, such as $\{++-+---+-+--+-\ldots\}$. Several physical magnitudes of interest can be obtained for any given state. Energy follows immediately from the Hamiltonian given by Eq. (1), where satisfied exchange interactions contribute with $-J$ to the energy, while frustrated exchange interactions contribute with $+J$. Not all interactions can be satisfied even for a ground state, so energies are usually higher than $-3N$, which would be the case for a fully unfrustrated system like the pure F case ($x=0.0$). The degeneracy of the ground manifold is usually very large and it is formed by clusters of states separated by energy barriers [11,12]. To simplify notation, energies will be expressed in units of J.

The magnetization of the system is just the addition of all magnetic moments. Except for a multiplicative constant the magnetization per site can be written in the following simplified way:

$$M = \left| \frac{1}{N} \sum_{i}^{N} S_i \right|. \tag{2}$$

The absolute value indicates that we are interested in a net magnetization regardless of any particular orientation.

The magnetic susceptibility is also a useful observable for this problem, it can be defined as

$$\chi(x,L,T) = N \frac{\langle M(x,L,T)^2 \rangle - \langle M(x,L,T) \rangle^2}{T}. \tag{3}$$

The magnetization is not a good observable to characterize all the phases present for the full range of x. Then, the instantaneous site order parameter $q(t)$ known as Edwards–Anderson parameter is preferred [13]. This can be defined as

$$q(t) = \left| \frac{1}{N} \sum_{i}^{N} S_i(0) S_i(t) \right|, \tag{4}$$

where $S_i(0)$ is the spin orientation at an arbitrary initial time after equilibration and $S_i(t)$ is the orientation of the same site after a time t. Since the Hamiltonian is symmetric with respect to the simultaneous inversion of all spins we will use the absolute value of $q(t)$ which is equivalent to work on half of the configuration space all the time.

2.2. Monte Carlo simulations

We will use Glauber dynamics visiting sites at random and testing the change in energy ΔE after flipping the spin at each site [14]. If energy decreases or remains the same ($\Delta E \leq 0$), the spin-flip is accepted and the system is characterized by the new state. However, even if energy increases ($\Delta E > 0$) we still accept the evolution to the new state provided $\exp(-\Delta E/T) > r$, where r is a randomly generated number in the range $[0.0, 1.0]$. This aleatory process is known as Metropolis algorithm. Temperature and energy are measured in units of the exchange constant J. One Monte Carlo step (MCS) is reached after N spin flip attempts. Time is then measured in units of MCS. Instants and intervals can be defined at integer number of MCS. The definition of the initial time $t=0$ is critical specially at low temperatures where the system finds difficulties to evolve to a true ground state by means of the slow MC process. However, this is not the main issue here as we will show that the method based on information theory is not extremely affected by equilibration. Actually this is one of the main new results reported below. So we will not need to search for methods or perform extremely long evolutions to recognize the phase transition.

Time evolution will be handled as previously defined in the literature [1] in a process that can be summarized in the following way. Several samples for a given concentration x are randomly prepared; one sample at a time is subject to the simulation described next. Temperature T is defined, varying from 0.1 to 5.0 generally speaking. Then a random state is picked and equilibration begins and goes on for 10 000 MC steps. Then the initial time $t=0$ is defined. From here on the system continues to evolve and energy $E(t)$, magnetization $M(t)$ and site order parameter $q(t)$ are calculated. All these magnitudes are recorded at intervals of 20 MCS. Results of the simulations were stored as vectors with values for 120 000 of such instants meaning a total of 2 400 000 MCS for each sample, of each size, of a given concentration and at a given temperature. The full vector was used for the crossing analyses below. In the case of the file compression method it was enough to consider 30 000 of such instants (600 000 MC steps) as already established in the previous works [2]. These extensive numeric calculations find a limitation in a maximum size for the systems under consideration. However, using the sizes analyzed here clear tendencies towards the thermodynamic limit are appreciated.

Different regimes are apparent depending on the concentration and temperature which is reflected in the amount of information content of the files storing the time sequence of any observable. Thus for instance, for $x=0.125$, where a critical temperature T^* slightly over 3.2 will be reported below, three different regimes for $q(t)$ are found: under, around and over T^*. Under T^* the order parameter does not change much, tending to keep a fixed constant value, situation that is favored at very low temperatures; the time sequence stored tends to repeat nearly the same information for long periods of time favoring data compression. For temperatures higher than T^*, evolution tends to follow the random choice of the Metropolis algorithm since most of the flip attempts are accepted; this means that q tends to oscillate around zero in a monotonous way repeating the small values of the observable in the short run which also favors compression but differently than in the previous case. In the intermediate case, for $T \approx T^*$, the system switches chaotically from one state to next, yielding sequentially different large values of any observable meaning high information content which makes the corresponding sequential data files very hard to compress. In this way, near the critical temperature the information content tends to maximize.

3. Results and discussion

Results are arranged in the following way. We begin by presenting ways of determining transition temperatures based on well-known methods to validate the sets of samples used later on when applying the new method based on information content. All these results bear in common some general features:

(a) Sample sizes are varied from $L=16$ to $L=36$.
(b) For each size L several concentrations x are considered in the range $[0.0, 0.5]$; the rest of the interval is equivalent to this one due to the symmetry of the Hamiltonian with respect to $x=0.5$.
(c) For each L and x several equivalent randomly generated samples were studied. A sample is one particular bond distribution for fixed L and x values.
(d) Temperature T is defined, varying it from 0.1 to 5.0 generally speaking, although emphasis is always near the critical temperature obtained in this way, which we will designate by T^*.

(e) Each sample was initiated at a random state; then the system was let to equilibrate for 10 000 MC steps. Then the system runs over for 2 400 000 MC steps. Values of observables for each sample at given L and x values correspond to the average of the 120 000 values recorded at intervals of 20 MC steps.
(f) The final values for magnetization, correlation functions, site-order parameter and other parameters reported below correspond to average values for 30 equivalent samples for given sets of L and x.
(g) The sequence for each of the simulated parameters were stored as vectors with 120 000 entries. This was done for each sample, each L, for each x and also for each simulated temperature T.

Files for the different observables were then processed in the way presented below in this section. Before going onto the new method we consider the well established crossing methods. The idea is to use these same samples to then invoke the new method based on data compression obtaining some new results; in the case of confirmation of previous results advantages of the new method will be brought out. So we begin by briefly reviewing the application of the traditional methods.

3.1. Crossing methods

Binder cumulant crossing techniques have been used to characterize ferromagnetic to paramagnetic transitions in these systems [15]. The cumulant for any observable Q whose distribution of possible results is known is defined as

$$\Psi(x,L,T)=1-\frac{1}{3}\frac{|\langle Q^4\rangle_{xLT}|_M}{|\langle Q^2\rangle_{xLT}|_M^2}, \tag{5}$$

where $\langle\cdot\rangle_{xLT}$ means an average for the sequence of a given sample at a given T; then an average of these values over the set of M equivalent randomly generated samples is considered.

Here we will also use an alternative way by means of the crossing of autocorrelation functions [1,2], since to our knowledge this technique has not been applied to 3D systems so far. We make use of the following relationship to define the time autocorrelation function (TAF) to be used below:

$$C(x,L,T,\tau)=\frac{\nu}{\nu-\tau}\frac{\sum_{t=0}^{\nu-\tau}Q(t)Q(t+\tau)}{\sum_{t=0}^{\nu}Q(t)Q(t)}, \tag{6}$$

where $Q(t)$ can be any observable at instant t and τ is the time separation over which the correlation is to be established. The span for τ was 10 000 MCS which allows to average over a great amount of initial instants for the same τ. An average $\langle C(x,L,T)\rangle$ over all these intervals is then obtained as representative of the time autocorrelation function for a sample of a given concentration x, size L, at the simulation temperature T. Then the average value over the M samples is calculated.

Let us consider the Edwards–Anderson site order parameter defined in Eq. (4) as the variable for BC and TAF, namely, $Q(t)=q(t)$. For the concentration $x=1/8=0.125$ we get the results shown in Fig. 1 for the sizes indicated in the insets of that figure. It is clear that all curves tend to cross for temperatures somewhere between 3.2 and 3.3. The same results holds both for Binder cumulants and autocorrelation functions.

When the same treatment is done for samples with $x=3/8=0.375$ a completely different picture is obtained as shown in Fig. 2. Now there is no clear crossing temperature. A different way to put it is that crossing temperatures are spread over a large range, meaning large error bars to any average that could be defined. Even if equilibration times are varied the problem persists. It is clear that crossing mechanisms (even more so for BC) are not appropriate to cope with any possible phase transition for $x=0.375$ and other similar concentrations. As it will shown below, a drastic change of regime is found for near $x^*\approx 0.22$.

The use of crossing methods will be limited to yield critical temperatures for $x\leq 0.22$ thus opening the possibility of investigating alternative methods which can complement the crossing methods; such method is presented below and it is based on data compression techniques. Once this method is established it will be used to obtain critical temperatures for the rest of the range of x.

3.2. Magnetization

To clearly characterize the difference between the two regimes identified in the previous section let us calculate the magnetization for the same two concentrations used above. In doing so we obtain the magnetization per site by means of Eq. (2); results for $x=0.125$ are shown in Fig. 3 for the sizes given in the inset. Magnetization goes to zero as T approaches $T^*=3.25$ approximately, thus indicating that this is a ferromagnetic to paramagnetic transition. The corresponding magnetic susceptibility can be calculated by means of Eq. (3) giving the usual sharp peak at the same temperature T^* as shown in Fig. 4.

When the same analysis is done for samples of the same size but for concentration 0.375 no ferromagnetic ordering is found. The absolute value of the magnetization is always close to zero effect which is more notorious as size increases. The corresponding magnetic susceptibility results are shown in Fig. 5. Although there is a broad maximum for temperatures between 0.7 and 1.5, there are strong oscillations for the values of susceptibility and no

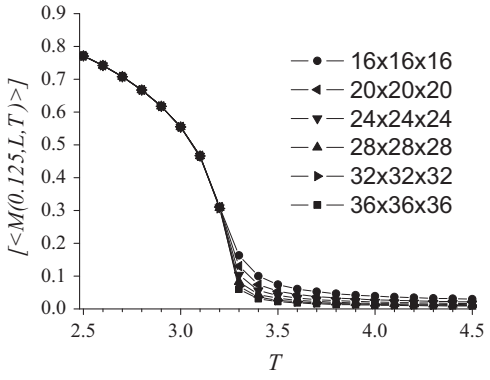

Fig. 3. Magnetization as function of temperature T for concentration $x=0.125$; sizes are shown in the inset.

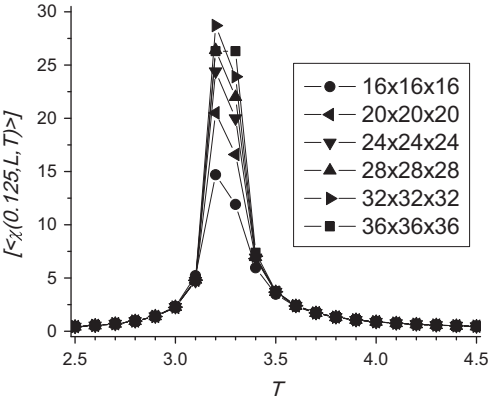

Fig. 4. Magnetic susceptibility (arbitrary units) as function of temperature for. Sample sizes are given in the inset. There is a clear indication for a ferromagnetic to paramagnetic transition around $T=3.25$.

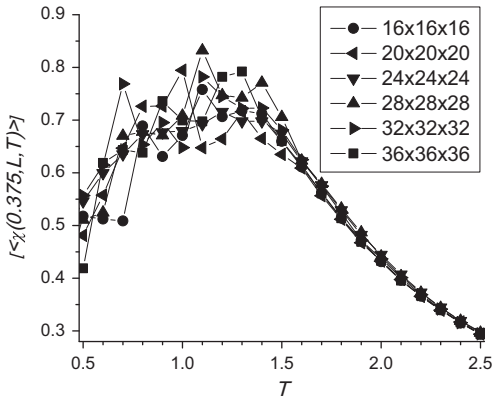

Fig. 5. Magnetic susceptibility (arbitrary units) as function of temperature for concentration 0.375. Sample sizes are given in the inset. There is no clear single critical temperature although the indication for a spin-glass to paramagnetic transition is present.

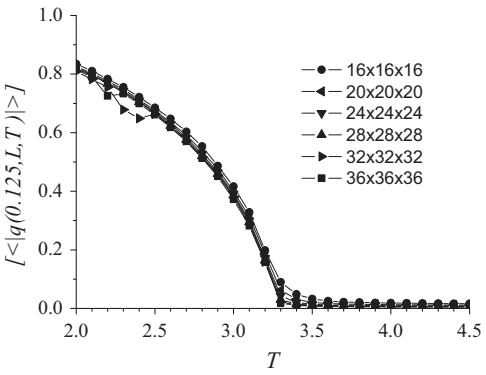

Fig. 6. Behavior of site order parameter q for concentration $x=0.125$, for the sizes given in the inset; $|q|$ shows a behavior similar to the magnetization in Fig. 3, pointing to vanish near 3.25.

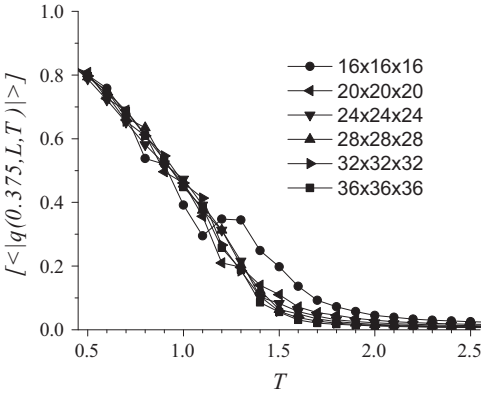

Fig. 7. Behavior of site order parameter q for two concentration $x=0.375$ showing a tendency to vanish near 1.3; such effect is not observed in the case of the magnetization of these samples. This indicates that the transition at the higher concentration corresponds to the transit of a spin-glass phase to a paramagnetic phase.

clear tendency with increasing size can be noticed. From these results it is not possible to obtain a critical temperature for a possible transition from a spin-glass phase to a paramagnetic phase. Eventually these results can be improved with a better equilibration, but this is not the idea here. On the contrary, we want to preserve these data and use the same information generated in this way when we deal with the data compressor method in the corresponding subsection below. Thus, we will be able to appreciate one of the advantages of the new method: it is not so sensitive to equilibration mechanisms.

3.3. Site order parameter

Following the same spirit of the previous subsection we present now the results for Edwards–Anderson parameter using Eq. (4). Fig. 6 presents the results for the absolute value of q as a function of temperature for $x=0.125$ and for the sizes given in the inset, showing a behavior quite similar to the magnetization in Fig. 3. Except for small size effect the EA site order parameter functions tends to vanish somewhere slightly over 3.2.

When the same procedure is applied to samples of concentration 0.375 the behavior of Edwards–Anderson parameter now differs from that of the magnetization as shown in Fig. 7. Except for a few instabilities attributable to small size lattices, the site-order parameter vanishes as temperature is raised, showing that there is an ordering for low enough temperatures. Although it is hard to estimate such temperature due to the prevailing tails usual for finite size lattices, the transition temperature is clearly under 1.4. The important point here is to establish that there is magnetic ordering for concentration 0.375 and that this is well represented by the simulations obtained for the samples under consideration. The question now is whether the method based on data compression recognizes this ordering yielding a value for the transition temperature.

3.4. Information content

Most of the previous results are known in general with the exception of the application of the crossing of autocorrelation functions to 3D systems (right-hand side of Figs. 1 and 2). The reason to review these results numerically here is to make sure the sets of samples generated in the way described in the introduction behave as expected. In this way the application of the method of data compression will be tested using the same samples and the same data as for the other methods. This will also allow a discussion of the characteristics and advantages of the new method.

The details of the method, including an example of the way it works, are given somewhere else [2] so here we give just the essentials to immediately apply the method. We consider the same files $Q(t)$ described above when dealing with time-autocorrelation functions but it is enough to consider the leading 30 000 instants separated by 20 MC steps [2]. This marks already a large difference with the previous methods where long time series have to be considered to better stabilize the results when possible. Here $Q(t)$ can be any observable for the system. However, it was already shown that for Ising systems compression of the files containing the absolute value of the Edwards–Anderson parameter give the best results for these frustrated systems. So from now on we will deal exclusively with the files for $q(x,L,T,t)$ generated via Monte Carlo (MC) simulation for cubic samples of size $N=L\times L\times L$, with a concentration x of A bonds, at a fixed temperature T storing data sequentially in time t.

Such truncated files (30 000 instants) are then compressed using wlzip; the compressed files are designated by $q^*(x,L,T)$ where the important parameter here is its weight in bytes (B) or kilobytes (kB) designated by $w(x,L,T)$. In Fig. 8 we plot $w(0.125,L,T)$ as a function of T for the sizes given in the inset. Several comments are in order. First, the compression reached by the files is clearly dependent on temperature. Second, all curves tend to maximize at approximately the same temperature independent of lattice size. Third, contrast increases with lattice size. Fourth, sharpness also increases with size suggesting that in the thermodynamic limit the curve will approach something similar to

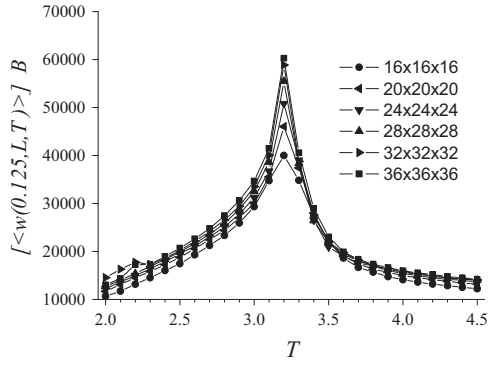

Fig. 8. Average weight of compressed files for the absolute value of parameter q for concentration $x=0.125$ and for the sizes given in the inset. A clear tendency for a transition temperature close to 3.2 is observed.

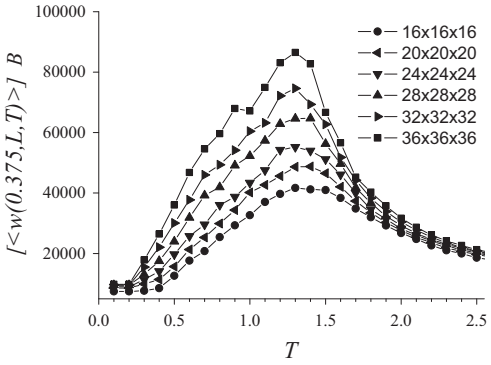

Fig. 9. Average weight of compressed files for the absolute value of parameter q for concentration $x=0.375$. Lattice sizes given in the inset. Although less sharp that in Fig. 8, curves indicate a maximum near $T=1.3$ for all lattice sizes.

a delta function. Fifth, for the particular concentration under consideration we can say that curves tend to maximize at a temperature $T^* \approx 3.2$, in good agreement with Figs. 4 and 6.

When the same procedure is applied to samples of concentration 0.375 the results for the compression produce distinct curves as presented in Fig. 9. The right-hand side (higher T) of these curves are similar to the corresponding ones for $x=0.125$ presented in the previous figure. However, there are differences at the center and on the left-hand side: a broad well defined maximum is now observed. We investigated if larger equilibration times or longer times series could lead to a sharper transitions but this is not the case. On the contrary, the general shape of these curves remains the same even if we cut the time series from the 240 000 instants to only 30 000 which is what was used to plot Fig. 9. Then we have to consider that the broad curves are intrinsic to the determination of spin-glass to paramagnetic transitions, while sharp curves correspond to ferromagnetic to paramagnetic transitions.

At this point it is useful to compare Fig. 9 to Fig. 5, which are based on data generated sequentially by the same MC process. The following differences favor the method of data compression: (a) although both families of curves are broad, those in Fig. 9 are a bit sharper; (b) in Fig. 9 each size produced a clearly different curve; (c) for each size in Fig. 9 there is a maximum; (d) the temperature of the maxima tends to migrate smoothly from 1.4 for $L=16$ to 1.3 for $L=36$, with an indication to approach slightly lower values for larger sizes; (e) with this analysis we can report a critical temperature of $T^* \approx 1.3$ or slightly underneath for the critical temperature at concentration $x=0.375$; (f) to obtain Fig. 9 data for only 30 000 instants were needed which means that the method of data compression needs less computer time than other methods to obtain useful results. If 15 000 or less instants are used the tendencies shown in Fig. 9 are smeared out as random oscillations in the data begin to appear.

This empirical test validates the data compression method to recognize spin-glass to paramagnetic transitions where magnetization and crossing methods fail. Moreover, equilibration appears to be non-critical for this process; even short time series allow to recognize clear maxima in all the curves. This is a notorious advantage of the new method reported here with respect to other methods. A possible reason for this rapid convergence is discussed below.

A concentration requiring special attention is $x=0.5$ since there is abundant information in the literature for the corresponding critical temperature. In Fig. 10 we present results for several lattice sizes. The curves here look very alike to those of Fig. 9, thus confirming that S to P transition produces broader curves than those for F to P transition. Similarly to the previous concentration all curves tend to maximize near 1.3. This is slightly higher than the values reported in the literature: 1.20 [6,16,17], 1.195 [18], 1.19

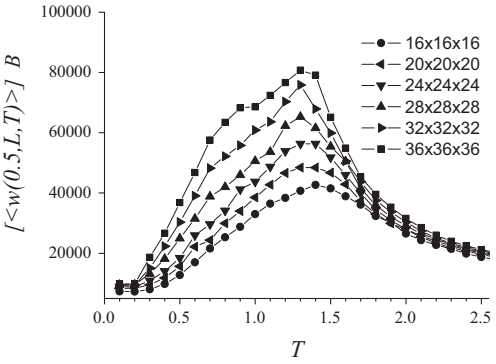

Fig. 10. Results of compression for the concentration $x=0.5$ and for the lattice sizes are shown in the inset. All curves maximize near 1.3 indicating a critical behavior close to that temperature.

[19], 1.175 [20], 1.7 [21]. 1.165 [22], 1.120 [23], 1.11 [24]. Apparently, in its present form compression by wlzip yields precise critical temperatures for ferromagnetic (F) to paramagnetic (P) transitions while it gives a rough approximation for the transition temperature when the spin-glass phase is involved. However, even in this last case, general shape of the curves in Fig. 9 is very robust for over 30 000 instants in the times series used for the compression.

We now focus our attention to the intermediate concentration zone where a triple point is expected: F, S and P regimes should come together at certain x^* and T^* values. To cope with this task we vary the concentration x at fine intervals within the range [0.1875, 0.25] (equivalent to [3/16, 1/4]): for each such x we vary T as before. Results for $L=32$ are presented in Fig. 11. Several comments are in order: (i) curves clearly maximize indicating phase transitions; (ii) curves for $x \approx 0.2$ present two maxima indicating reentrance; (iii) for each of such curves the high temperature transition is sharper (F to P) while the low temperature transition (possibly F to S) is broader; (iv) the tripple point seems to be near to $x \approx 0.22$ and $T \approx 1.6$; (v) the fact that the same sample for any given x just under the triple point produces a sharp curve for the F to P transition while it produces a broader curve for the transition involving the S phase (under the same simulation conditions) shows that the shape of the curve is an indication of the kind of phase transition involved; (vi) the reentrant behavior found here is a general feature in systems where competing interactions and frustration are present [9,10,25] which is precisely the case here.

Let us single out the intermediate curve for $x = 27/128 = 0.2109375$, whose right-hand side is similar to all curves including those at lower concentrations. It can be also noticed that the left-hand side of this same

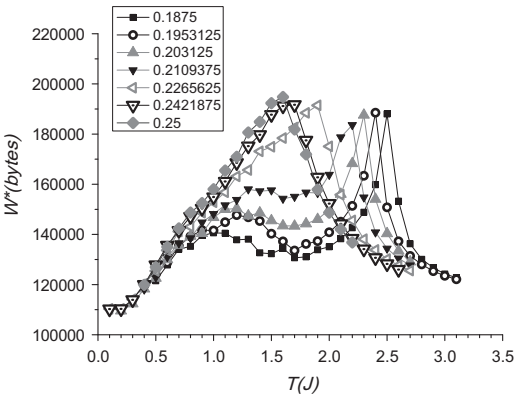

Fig. 11. Compression for files of size $L=32$ for the different concentrations x given in the inset. Clearly two behaviors are observed: for concentrations $x>0.22$ broad curves like those in the two previous figures are produced; for $x<0.2$ curves with both a sharp and narrow peak are obtained at high T and a broader maximum is also present at lower T values. This is a clear indication for a reentrance as discussed in the text.

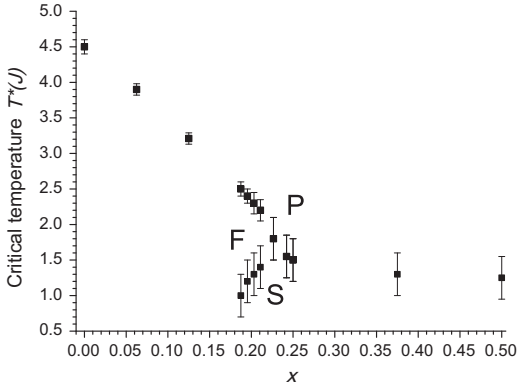

Fig. 12. Phase diagram obtained using wlzip for the lattice size $L=32$. For concentrations of A bonds in the range $0.22<x\leq 0.50$ no magnetization is present and the transition corresponds to spin glass (S) to paramagnetic (P). Just under $x*\approx 0.22$ the system presents a S phase at low T, then a F phase as T increases ending in an P phase at larger temperatures which means the presence of a reentrance. For lower values of x a direct transit from a F phase to a P phase is found. The sectors marked as F, S and P in the diagram correspond to ferromagnetic, spin-glass and paramagnetic respectively.

curve is similar and almost coincident with curves for higher concentrations. Previous comments lead to the proposal that this structure is formed by two curves: a sharp one maximizing near 2.2 and a broad one maximizing at lower temperature. Actually this broad structure persists for lower concentrations until it disappears for x close to 0.18. On the other hand, for concentration $x=0.2265625$ is barely appreciated as a shoulder on the left-hand side of the curve, which disappears for the following concentrations. All of this discussion points to a reentrance of the ferromagnetic phase into the spin-glass phase. Reentrance is a general feature in systems where competing interactions and frustration are present [9,10,25] which is precisely the case here.

The extent of the reentrance towards low concentrations seems lo be larger here than expected from the results in the literature [9,25,26]. At the moment we find no explanation for this difference except that our results are based on a different method bearing an important error in the determination of the S to F transition since it is based on a broad weaker maximum mounted on the lower temperature side of a better defined maximum. Actually error bars in Fig. 11 are just indicative of what they could be as compared with the smaller ones which are observed in the case of the F to P transitions.

Previous analysis allows to draw a phase diagram for these systems based entirely on the method of data compression. This is done in Fig. 12 for size $L=32$. Except for the feature of the reentrance, this phase diagram is similar to other diagrams available in the literature obtained by different methods [7,8]. The error bars included in this figure are estimated from the half-width of the broad maxima in the previous figures. As it can be seen whenever the S phase is lost due to increase of temperature the transition is broad in temperature. However, transitions from F to P states are sharper as shown in Fig. 12 by smaller error bars.

Let us go back for a moment to the comparison of Figs. 5 and 9 emanated from the same data generated by computer simulations. How come the method of data compression gives better information than the magnetic susceptibility? We believe the reason is that magnetic susceptibility is based on the distribution of values collected along a large number of instants, but the time evolution is lost. In the case of the data compression the values are exactly the same as previous ones but the sooner a value repeats itself along the sequence of values the larger the compression achieved. That is to say, wlzip is designed to recognize meaningful physical information along the simulation time, which is wiped out in the calculation of magnetic susceptibility. This is also the reason to require less simulation time to produce meaningful curves with wlzip: the time-length needed is such that repetitions are clearly shown. Once this phenomenon saturates there is no point in considering larger time windows.

4. Conclusions

The method of data compression detects transitions from a ferromagnetic phase to a paramagnetic phase, as well as from a spin-glass phase to a ferromagnetic phase or to a paramagnetic phase. It can even recognize reentrance phenomena dealing with these three phases. This is very powerful because other methods give only partial description of these phase transitions.

There are differences in the way this method recognizes the possible transitions. The change of the extremely ordered ferromagnetic phase onto a phase without order at all – like the paramagnetic one – leads to sharp curves of data compression reflecting huge difference in information content between files describing properties of these two different phases. The change of the spin-glass phase onto a different phase is not so sharp since in this phase there is partial ordering: then broader curves of information content versus temperature are obtained. This means that the shape of the curve could be used to identify the kind of transition in the case of an unknown change of regime.

The recognition of a maximum in the compression ratio of the time series associated to the order parameter is not strongly dependent of the equilibration procedure. This is a clear advantage of this method.

For concentrations $x<0.22$ (or similarly for $x>0.78$) transitions from ferromagnetic (or antiferromagnetic) to paramagnetic phases are obtained with the transition temperature T^* varying from 4.51 at $x=0.0$ to near 1.6 at the triple point. Then for $x>0.22$ the critical temperature decreases slowly to near 1.3 for values $x=0.375$ or even less. Such critical temperature remains unchanged as it approaches $x=0.5$. Let us recall that the critical temperatures for the S to P transitions are subject to larger indetermination as compared to those obtained for the sharper F to P transitions.

All results by data compression reported here required modest simulation times of 600 000 MC steps, storing instants every 20 MC steps (30 000 instants). Although simulation with longer times could improve very slightly previous results the idea here is to show the robustness of this method, which require less computer time than others to recognize criticality.

The application of this method to other fields, such as econophysics, is also under way. Thus the application of wlzip to the

recognition of trends in stock markets has shown to produce valuable information [27]. Application to biomedical data is also under way. Generally speaking, the method of data compression can be applied to any time series or sequence to recognize repetitions or near repetitions thus characterizing different regimes for the system.

Acknowledgements

Partial support from the following three Chilean sources is acknowledged: Fondecyt under contract 1100156, Millennium Scientific Nucleus "Basic and Applied Magnetism" under contract P-06-022-F, Financiamiento Basal para Centros Científicos y Tecnológicos de Excelencia (Chile) through the Center for Development of Nanoscience and Nanotechnology (CEDENNA) (Basal Project FB0807). We thank helpful discussions with H. Katzgraber concerning reentrance.

References

[1] E.E. Vogel, G. Saravia, F. Bachmann, B. Fierro, J. Fischer, Physica A 388 (2009) 4075.
[2] E.E. Vogel, G. Saravia. V. Cortez, Physica A 391 (2012) 1591.
[3] D.G. Luenberger, Information Science, Princeton University Press, Princeton, NJ, Oxford, 2006.
[4] T.M. Cover, J.A. Thomas, Elements of Information Theory, 2nd edition, John Wiley & Sons, New York, 2006.
[5] J.G. Roederer, Information and its Role in Nature, Springer, Heidelberg, 2005.
[6] A.T. Ogielski, I. Morgenstern, Phys. Rev. Lett. 54 (1985) 928.
[7] Y. Ozeki, H. Nishimori, J. Phys. Soc. Jpn. 56 (1987) 1568.
[8] M. Hasenbusch, A. Pelissetto, E. Vicari, Phys. Rev. B 78 (2008) 214205 (and references therein).
[9] G. Ceccarelli, A. Pelissetto, E. Vicari, Phys. Rev. B 84 (2011) 134202.
[10] T.P. Toldin, A. Pelissetto, E. Vicari, J. Stat. Phys. 135 (2009) 1039–1061.
[11] J.F. Valdes, J. Cartes, E.E. Vogel, S. Kobe, T. Klotz, Physica A 257 (1998) 557.
[12] F. Roma, S. Risau-Gusman, A.J. Ramirez-Pastor, F. Nieto, E.E. Vogel, Phys. Rev. B 82 (2010) 214401.
[13] S.F. Edwards, P.W. Anderson, J. Phys. F: Met. Phys. 5 (1975) 965.
[14] R.J. Glauber, J. Math. Phys. 4 (1963) 294.
[15] K. Binder, Z. Phys. B 43 (1981) 119.
[16] R.R.P. Singh, S. Chakravarty, Phys. Rev. Lett. 57 (1986) 245.
[17] R.N. Bhatt, A.P. Young, Phys. Rev. Lett. 54 (1985) 924.
[18] P.O. Mari, I.A. Campbell, Phys. Rev. B 65 (2002) 184409.
[19] M. Pleimling, I.A. Campbell, Phys. Rev. B 72 (2005) 184429.
[20] A.T. Ogielski, Phys. Rev. B 32 (1985) 7384.
[21] T. Nakamura, S.-i. Endoh, T. Yamamoto, J. Phys. A 36 (2003) 10895.
[22] L.W. Bernardi, S. Prakash, I.A. Campbell, Phys. Rev. Lett. 77 (1996) 2798.
[23] H.G. Katzgraber, M. Körner, A.P. Young, Phys. Rev. B 73 (2006) 224432.
[24] N. Kawashima, A.P. Young, Phys. Rev. B 53 (1996) R484.
[25] C.K. Thomas, H.G. Katzgraber, Phys. Rev. B 84 (2011) 174404.
[26] A.K. Hartmann, Phys. Rev. B 59 (1999) 3617.
[27] E.E. Vogel, G. Saravia, Eur. Phys. J. B 87 (2014) 177. http://dx.doi.org/10.1140/epjb/e2014-41003-0.